

Mass gap in the 2D O(3) non-linear sigma model with a $\theta = \pi$ termB. Allés^a, A. Papa^b^a*INFN Sezione di Pisa, Pisa, Italy*^b*Dipartimento di Fisica, Università della Calabria and
INFN Gruppo Collegato di Cosenza, Arcavacata di Rende, Cosenza, Italy***Abstract**

By analytic continuation to real θ of data obtained from numerical simulation at imaginary θ we study the Haldane conjecture and show that the O(3) non-linear sigma model with a θ term in 2 dimensions becomes massless at $\theta = 3.10(5)$. A modified cluster algorithm has been introduced to simulate the model with imaginary θ . Two different definitions of the topological charge on the lattice have been used; one of them needs renormalization to match the continuum operator. Our work also offers a successful test for numerical methods based on analytic continuation.

1 Introduction

Several years ago Zamolodchikov and Zamolodchikov introduced an integrable S -matrix for massless particles which was associated to the 2-dimensional $O(3)$ non-linear sigma model with a topological θ term for $\theta = \pi$ [1].

Therefore the 2-dimensional $O(3)$ sigma model with $\theta = \pi$ is possibly gapless. Actually this conclusion was previously achieved by Haldane and Affleck. They worked out a low energy description of the 1-dimensional chain of quantum half-integer spin with antiferromagnetic coupling finding that it and the above-mentioned $O(3)$ sigma model share the same long distance properties [2, 3, 4]. Moreover it was found that antiferromagnetic quantum spin chains are gapless for half-integer spins [2, 5].

Later Affleck and Haldane [6] argued that the critical theory for the half-integer quantum antiferromagnetic spin chain is the Wess-Zumino-Witten model with a topological coupling $k = 1$. This model is the stable fixed point of the 2-dimensional $O(3)$ sigma model with a vacuum angle $\theta = \pi$.

In addition, two numerical calculations of the partition function for the $O(3)$ model in the presence of a θ term [7] yield indications that the theory undergoes a second order phase transition at $\theta = \pi$ (although the two analyses disagree about the universality class).

In the present work we introduce a direct numerical method to verify the Haldane conjecture for the 2-dimensional $O(3)$ non-linear sigma model. The idea is to perform a Monte Carlo study on the lattice of the mass gap in the model as a function of the θ parameter and to show that it vanishes at a precise value of θ , called θ_{end} , which, following Haldane, should be $\theta_{\text{end}} = \pi$. We overcome the sign problem by simulating the theory at imaginary θ and analytically continuing the results to the real θ values. To this end we introduce a new cluster algorithm that works for imaginary non-zero theta.

2 Lattice implementation

The continuum expression for the action of the model is

$$\begin{aligned} S &= A - i\theta Q, \quad A = \frac{1}{2g} \int d^2x \left(\partial_\mu \vec{\phi}(x) \right)^2, \\ Q &= \int d^2x Q(x), \end{aligned}$$

$$Q(x) \equiv \frac{1}{8\pi} \epsilon^{\mu\nu} \epsilon_{abc} \phi^a(x) \partial_\mu \phi^b(x) \partial_\nu \phi^c(x) , \quad (1)$$

where g is the coupling constant and $Q(x)$ is the topological charge density. $\vec{\phi}(x)$ is a 3-component unit vector that represents the dynamical variable at the site x . We have regularized this action on a square lattice by the expression

$$S_L = A_L - i\theta_L Q_L , \quad A_L \equiv -\beta \sum_{x,\mu} \vec{\phi}(x) \cdot \vec{\phi}(x + \hat{\mu}) , \quad (2)$$

where $Q_L = \sum_x Q_L(x)$ is the total lattice topological charge and $Q_L(x)$ is the lattice topological charge density. β is the inverse bare lattice coupling constant and θ_L is the bare vacuum angle. In general, $\theta_L \neq \theta$ and the point where the lattice regularized model becomes massless will be called $\theta_{L,\text{end}}$.

The action A_L used in (2) is the simplest one on the lattice. More complicated actions and expansion parameters boast better scaling and asymptotic scaling properties and hence they are more suited for the calculation of masses [8, 9, 10]. However our interest lies only on the vanishing of the mass gap at a particular value of θ_L and such a property is clearly unaffected by the slow convergence of the series.

3 Choice of Q_L

Let us discuss the regularization of the topological charge density to be used in our Monte Carlo simulation. Q counts how many times the configuration of spin variables winds around the unit sphere. Hence Q takes on integer values. Configurations with +1 (−1) winding number are called instantons (anti-instantons) [11].

We have made use of two different lattice regularizations for the topological charge density. The first one [12]

$$Q_L^{(1)}(x) \equiv \frac{1}{32\pi} \epsilon^{\mu\nu} \epsilon_{abc} \phi^a(x) \left(\phi^b(x + \hat{\mu}) - \phi^b(x - \hat{\mu}) \right) \cdot \left(\phi^c(x + \hat{\nu}) - \phi^c(x - \hat{\nu}) \right) , \quad (3)$$

is a symmetrical discretization of the expression for $Q(x)$ in Eq.(1).

The second lattice regularization is defined on triangles (not on single sites). Every plaquette of a square lattice can be cut through a diagonal

into two triangles. If we call $\vec{\phi}_1$, $\vec{\phi}_2$ and $\vec{\phi}_3$ the fields at the sites of the three vertices (numbered counter-clockwise) of one of these triangles then the fraction of spherical angle subtended by these fields is $Q_L^{(2)}(\Delta)$ which satisfies [13]

$$\exp\left(2\pi i Q_L^{(2)}(\Delta)\right) = \frac{1}{\rho} \left(1 + \vec{\phi}_1 \cdot \vec{\phi}_2 + \vec{\phi}_2 \cdot \vec{\phi}_3 + \vec{\phi}_3 \cdot \vec{\phi}_1 + i \vec{\phi}_1 \cdot (\vec{\phi}_2 \times \vec{\phi}_3)\right), \quad (4)$$

where $\rho^2 \equiv 2(1 + \vec{\phi}_1 \cdot \vec{\phi}_2)(1 + \vec{\phi}_2 \cdot \vec{\phi}_3)(1 + \vec{\phi}_3 \cdot \vec{\phi}_1)$ and $Q_L^{(2)}(\Delta) \in [-\frac{1}{2}, +\frac{1}{2}]$. The sum of $Q_L^{(2)}(\Delta)$ over all triangles yields the so-called geometric topological charge $Q_L^{(2)}$.

In general, a regularization of Q does not lead to integer values on a single configuration. To recover integer results for Q_L on ensembles of configurations that belong to the same topological sector, we must renormalize this operator. The lattice and the continuum topological charges are related by [14]

$$Q_L^{(1,2)} = Z_Q^{(1,2)} Q, \quad (5)$$

$Z_Q^{(1,2)}$ being the corresponding renormalization constant which is UV finite since the topological charge operator has no anomalous dimensions in the model under study.

$Z_Q^{(1,2)}$ can be calculated either in perturbation theory [14] or by a non-perturbative numerical method [15]. We have used the latter. In a nutshell it works in the following way: a classical instanton (with topological charge +1) is put by hand on the lattice and then 100 updating steps are applied (we used the Heat-Bath algorithm on the conventional O(3) non-linear σ model without a θ term since the renormalization constant to be used in Eq.(5) cannot depend on θ). After every Heat-Bath step the value of $Q_L^{(1,2)}$ is measured and, in order to monitor the background charge and check that it is not varied after the updating step, $Q_L^{(1,2)}$ is measured again after 6 cooling hits. In the calculation of $Z_Q^{(1)}$ this procedure was repeated $4 \cdot 10^4$ times at $\beta = 1.5$ and 1.6 and 10^4 times for $\beta = 1.7$ and 1.75 . The average of $Q_L^{(1,2)}$ on configurations within the topological sector +1 yields $Z_Q^{(1,2)}$.

The above non-perturbative method is summarized by the expression

$$Z_Q^{(1,2)} = \frac{\int_{1\text{-instanton}} \mathcal{D}\vec{\phi} Q_L^{(1,2)} \exp(-A_L)}{\int_{1\text{-instanton}} \mathcal{D}\vec{\phi} \exp(-A_L)}. \quad (6)$$

The restricted path integral runs over all configurations (fluctuations) that preserve the background of one instanton. Since the geometric charge $Q_L^{(2)}$ is +1 till the background classical configuration is one instanton (whatever the fluctuations are), the expression (6) yields $Z_Q^{(2)} = 1$ for all β [16].

The determination of $Z_Q^{(1)}$ is not so trivial and an example of such an evaluation is shown in Fig.1. Measures of $Q_L^{(1)}$ on configurations that belong to the topological sector +1 attain to a plateau (in general after a few Heat-Bath steps) and stay on it for the rest of the updating steps. The height of this plateau is the value of $Z_Q^{(1)}$. In Table 1 the results for $Z_Q^{(1)}$ at the values of β used in the present work are given.

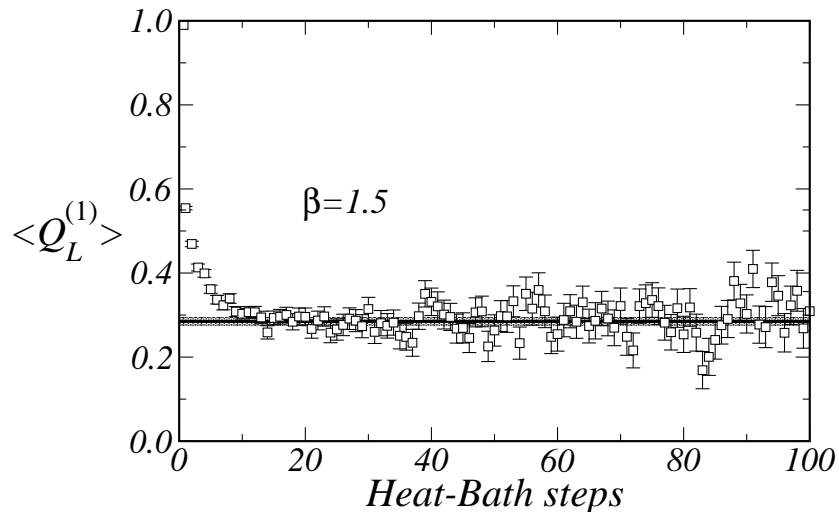


Figure 1: Data for $\langle Q_L^{(1)} \rangle$ start at +1 at the 0-th Heat-Bath step and then they go down until reaching a plateau. The horizontal line and grey band are the value and error respectively of $Z_Q^{(1)}(\beta = 1.5)$.

The relevant consequence of the above considerations for our study is that the vacuum angle θ is related to the corresponding bare parameter by the expression $\theta = \theta_L Z_Q^{(1,2)}$ (which implies $\theta = \theta_L$ when $Q_L^{(2)}$ is used).

4 Cluster algorithm for imaginary θ

Although the use of the topological charge density $Q_L^{(1)}$ requires the knowledge of a renormalization constant, it brings about the advantage that the action S_L in (2) can be simulated on the lattice by use of a fast cluster algorithm. Instead when the geometric charge $Q_L^{(2)}$ was used, the model was updated by a (rather slow) Metropolis algorithm.

Let us briefly describe the main characteristics of the new cluster algorithm expressly devised for the present work. The first part of an updating step with the usual Wolff algorithm [17] for the standard $O(3)$ sigma model without a θ term consists in choosing a random unit vector \vec{r} in such a way that every dynamical field can be split in a component parallel to \vec{r} and the rest, $\vec{\phi}(x) = (\vec{\phi}(x) \cdot \vec{r}) \vec{r} + \vec{\phi}_\perp(x)$, where $\vec{\phi}_\perp(x)$ denotes the part of $\vec{\phi}(x)$ orthogonal to \vec{r} . Then the signs of $(\vec{\phi}(x) \cdot \vec{r})$ for all x are updated à la Swendsen–Wang as in the Ising model [18].

By introducing the above separation for $\vec{\phi}(x)$ in the expression (3) we can re-write it as

$$\begin{aligned} Q_L^{(1)}(x) = & \frac{1}{16\pi} \left\{ (\vec{\phi}(x) \cdot \vec{r}) (d_{1,2} + d_{-1,-2} + d_{2,-1} + d_{-2,1}) \right. \\ & + (\vec{\phi}(x + \hat{1}) \cdot \vec{r}) (d_{0,-2} - d_{0,2}) + (\vec{\phi}(x - \hat{1}) \cdot \vec{r}) (d_{0,2} - d_{0,-2}) \\ & \left. + (\vec{\phi}(x + \hat{2}) \cdot \vec{r}) (d_{0,1} - d_{0,-1}) + (\vec{\phi}(x - \hat{2}) \cdot \vec{r}) (d_{0,-1} - d_{0,1}) \right\}, \quad (7) \end{aligned}$$

where $x \pm \hat{1}$ means the site at the position one step forward (backward) in the direction “1” starting from site x and the notation $d_{i,j}$ stands for the 3×3 determinant (the three components for each vector must be unfold along the rows)

$$d_{i,j} \equiv \det \begin{pmatrix} \vec{r} \\ \vec{\phi}(x + \hat{i}) \\ \vec{\phi}(x + \hat{j}) \end{pmatrix}. \quad (8)$$

In this fashion the theory at each updating step looks like an Ising model in the bosom of an external local magnetic field $h(x)$ because the expression in Eq.(7) is linear in $(\vec{\phi} \cdot \vec{r})$. Recall that all Monte Carlo simulations have been performed with an imaginary vacuum angle $\theta_L = +i\vartheta_L$, ($\vartheta_L \in \mathbb{R}$). By gathering all contributions of the type shown in Eq.(7) that contain $(\vec{\phi}(x) \cdot \vec{r})$

at site x one can readily derive the effective magnetic field at this site,

$$\begin{aligned}
h(x) = & -\frac{\vartheta_L}{16\pi} |\vec{\phi}(x) \cdot \vec{r}| \left(d_{1,2} + d_{-1,-2} + d_{2,-1} + d_{-2,1} \right. \\
& + d_{-1,-1-2} + d_{-1+2,-1} + d_{1,1+2} + d_{1-2,1} \\
& \left. + d_{2,2-1} + d_{2+1,2} + d_{-2,-2+1} + d_{-2-1,-2} \right). \quad (9)
\end{aligned}$$

$d_{i+k,j}$ (and analogous terms in (9)) are the straightforward generalization of the above definition (8) when the site is obtained by shifting two steps from the original position x , the first in the direction \hat{i} and the second in the direction \hat{k} .

Hence the last step in the updating consists in applying to the above expressions an algorithm valid for the Ising model in presence of a magnetic field. In the literature there are two such algorithms, the Lauwers–Rittenberg [19] and the Wang [20, 21] methods. After testing their performances and comparing the corresponding decorrelation times with the usual (multihit) Metropolis, Heat–Bath and overHeat–Bath, we decided for the Wang algorithm. It consists in placing the magnetic field on an extra, fictitious site (called ghost site) that couples to every Ising spin through the value of $h(x)$. Using this coupling on the same footing as all other terms in the action, the Fortuin–Kasteleyn clusters [22] are arranged by the Hoshen–Kopelman algorithm [23] and then updated with the usual $\frac{1}{2}$ probability.

Following the proof given in [17], it can be seen that our algorithm also satisfies the detailed balance property.

5 Results

Operators representing physical states can be built out of an arbitrary number of fundamental fields since supposedly the model is not parity invariant for $\theta_L \neq 0$. As the energy gap is given by the mass of a triplet state [24] we studied the correlation functions of operators having one O(3) index as quantum number,

$$\vec{\mathcal{O}}_1(x) \equiv \vec{\phi}(x), \quad \vec{\mathcal{O}}_2(x) \equiv \vec{\phi}(x) \times \vec{\phi}(x + \hat{1}). \quad (10)$$

Then we calculated the related wall operators by averaging over the x_1 coordinate (as usual L is the lattice size), $\vec{\mathcal{W}}_i(x_2) \equiv \frac{1}{L} \sum_{x_1} \vec{\mathcal{O}}_i(x)$ for $i = 1, 2$.

To single out the correct parity mixture for the physical particle and to clean the signal from possible excited states, we extracted the triplet mass m by using the variational method of Ref. [25] where the mass is obtained from the exponential decay of the largest eigenvalue of the correlation matrix $\langle \vec{\mathcal{W}}_i(x_2) \vec{\mathcal{W}}_j(0) \rangle - \langle \vec{\mathcal{W}}_i \rangle \langle \vec{\mathcal{W}}_j \rangle$.

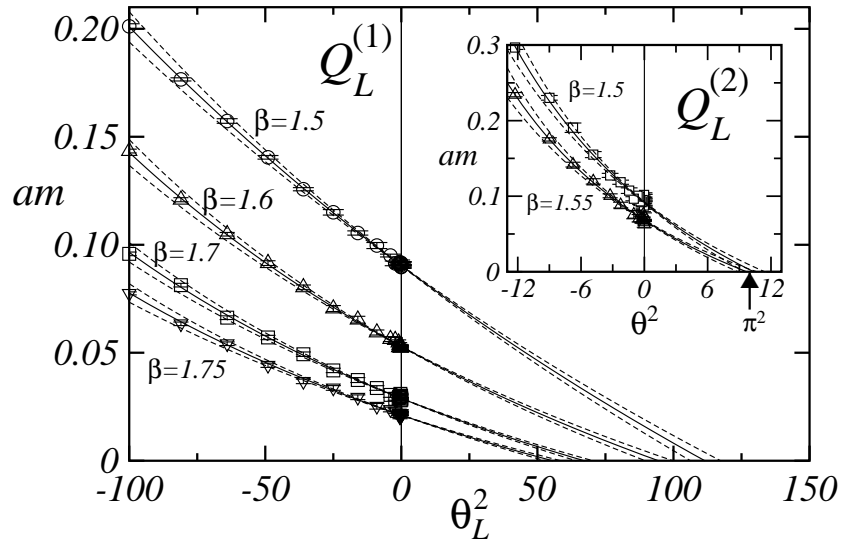


Figure 2: Behavior of the mass gap (in units of the lattice spacing a) as a function of θ_L^2 . Main plot: circles ($\beta = 1.5$), up triangles ($\beta = 1.6$), squares ($\beta = 1.7$) and down triangles ($\beta = 1.75$) are the data from the simulation at imaginary θ_L ($\theta_L^2 < 0$) by using the $Q_L^{(1)}$ lattice regularized topological charge. Each continuous line is the result of the extrapolation described in the text and the dashed lines enclose the boundary of its error. Inset: the same for the $Q_L^{(2)}$ regularization: squares ($\beta = 1.5$) and up triangles ($\beta = 1.55$). In this case $\theta = \theta_L$ and the position of $\theta = \pi$ is indicated.

5.1 Results for $Q_L^{(1)}$

$2 \cdot 10^5$ decorrelated propagators were measured for all values of β and θ_L . In the main plot of Fig.2 the results for the triplet mass are shown for four

values of β . The extrapolations in this figure were done by using the functional form $(c_1 + c_2 \theta_L^2)/(1 + c_3 \theta_L^2)$. We avoided using a functional form dictated by some theoretical argument, like one that for real or imaginary θ_L goes like $m(\theta_L) = c_1(c_2^2 - \theta_L^2)^{2/3}$ which is, up to logarithmic corrections, the Renormalization Group prediction, because such an analytic form implicitly assumes the vanishing of the mass at a precise value of θ . Instead we made the extrapolations with ratios of polynomials (which are contemporaneously both simple and very general functional forms) in order to leave room for any behaviour in the vacuum angle. The results of the analytic continuations are given in Table 1. The physical value of θ where the theory becomes gapless is given by $\theta_{\text{end}} = \theta_{L,\text{end}} Z_Q^{(1)}$. The numbers in the last column are in fair agreement with the prediction that the model becomes massless when θ equals π . Similar results (and χ^2) were obtained from degree 2 or 3 polynomials in θ_L^2 , while ratios of higher order polynomials proved to be statistically unlikely (their χ^2 was too large).

Table 1. Values of $Z_Q^{(1)}$ and θ_{end} .

β	L	$(\theta_{L,\text{end}})^2$	$Z_Q^{(1)}$	$\chi^2/\text{d.o.f.}$	θ_{end}
1.5	120	111(5)	0.285(9)	0.90	3.00(12)
1.6	180	94(5)	0.325(6)	0.45	3.15(10)
1.7	340	67(3)	0.380(6)	1.04	3.11(9)
1.75	470	56(3)	0.412(5)	0.68	3.08(9)

The lattice sizes in Table 1 were chosen large enough to meet at $\theta_L = 0$ the condition $L/\xi \equiv L \cdot am \geq 10$. Once this inequality holds at $\theta_L = 0$, it is amply realized at the values of θ_L where the simulations were performed as inferred from Fig.2. This fact warrants the absence of significant finite size effects.

5.2 Results for $Q_L^{(2)}$

In this case a Metropolis algorithm was used for updating and 10^5 independent propagators were measured for each value of θ (recall that in the present case $\theta_L = \theta$). We report data for two values of β . They are displayed in the

inset of Fig.2. The value of θ where Haldane predicted the closing of the mass gap is indicated with an arrow, $\theta^2 = \pi^2$. The numerical results are given in Table 2. Comments similar to the $Q_L^{(1)}$ case apply to the extrapolations shown in the figure. Again the results are in fair agreement with the conjecture.

Table 2. θ_{end} for the operator $Q_L^{(2)}$.

β	L	$(\theta_{\text{end}})^2$	$\chi^2/\text{d.o.f.}$	θ_{end}
1.5	110	10.4(1.0)	1.72	3.22(16)
1.55	150	9.7(1.0)	0.73	3.11(16)

By averaging all results for both topological charge operators and assuming gaussian errors we obtain that the mass gap vanishes at $\theta_{\text{end}} = 3.10(5)$.

6 Conclusions

We have simulated the $O(3)$ non-linear sigma model in 2 dimensions with an imaginary θ term at several values of the lattice coupling β . The mass gap was measured and extrapolated towards real θ . In all cases the extrapolation vanished at a value of θ compatible with the Haldane conjecture $\theta = \pi$. Our result is $\theta = 3.10(5)$ which agrees within errors with the conjecture. This value seems very robust as it is independent of the topological charge density operator chosen for the simulation. In particular, an operator $Q_L^{(1)}$ that requires a non-trivial renormalization constant leads to the same conclusion than another operator (the geometric charge $Q_L^{(2)}$) that does not renormalize.

A new fast cluster algorithm was purposely introduced to simulate the theory with an imaginary θ term. It works for the operator $Q_L^{(1)}$. Instead, when the geometric topological charge $Q_L^{(2)}$ was used, the theory was simulated by a (rather slow) Metropolis algorithm.

A salient outcome of our work is the good performance of the analytic continuation from imaginary to real θ . No theoretical prejudices were assumed in the functional form used in the continuation, apart from the obvious requirement that it is analytic. This can be justified by a comparison with the

phase diagram shown in Ref. [26]. In the case of the geometrical charge our largest β and $\theta = \theta_L$ (1.55 and 3.5 respectively) are very far from the line of phase transitions; as for the $Q_L^{(1)}$ case, our largest β and $\theta = \theta_L Z_Q^{(1)}$ were 1.75 and 4.1, which again lie very far from any line of singular points.

The need to perform Monte Carlo simulations at imaginary values of θ is actually a blessing in disguise since it forced us to work at very small correlation lengths, as can be clearly seen in Fig.2. Had we studied the theory directly at real θ values, we would have met with severe finite size effects.

A key ingredient for the successful extrapolation was to have got data from simulations within a wide range of (imaginary) values of θ_L for all β , ($\vartheta_L \equiv -i\theta_L \in [0, 10]$ when $Q_L^{(1)}$ was used and $\vartheta_L = \vartheta \equiv -i\theta \in [0, 3.5]$ for $Q_L^{(2)}$, the difference of intervals being due to the effect of the non-trivial renormalization that must be applied to the former). All that looks encouraging for the numerical studies based on the analytic continuation with respect to a parameter in the theory, such as in QCD with non-zero chemical potential [27].

7 Acknowledgements

We thank Ettore Vicari and Adriano Di Giacomo for a critical reading of a preliminary draft of the paper and Giuseppe Mussardo for illuminating conversations. We also want to thank Gerrit Schierholz for valuable comments. A.P. thanks Domenico Giuliano for useful discussions.

References

- [1] A. B. Zamolodchikov, Al. B. Zamolodchikov, Nucl. Phys. B379, 602 (1992).
- [2] F. D. M. Haldane, Phys. Lett. A93, 464 (1983); Phys. Rev. Lett. 50, 1153 (1983).
- [3] I. Affleck, Nucl. Phys. B257, 397 (1985).
- [4] R. Shankar, N. Read, Nucl. Phys. B336, 457 (1990).

- [5] I. Affleck, E. H. Lieb, *Lett. Math. Phys.* 12, 57 (1986); for spin $\frac{1}{2}$ see also E. H. Lieb, T. Schultz, D. Mattis, *Ann. Phys.* 16, 407 (1961).
- [6] I. Affleck, F. D. M. Haldane, *Phys. Rev. B* 36, 5291 (1987).
- [7] W. Bietenholz, A. Pochinsky, U.–J. Wiese, *Phys. Rev. Lett.* 75, 4524 (1995); V. Azcoiti, G. Di Carlo, A. Galante, *Phys. Rev. Lett.* 98, 257203 (2007).
- [8] G. Parisi, in *Proc. XXth Int. Conf. on High Energy Physics*, ed. L. Durand, L. G. Pondrom, Madison, WI (1980); G. Martinelli, G. Parisi, R. Petronzio, *Phys. Lett.* B100, 485 (1981).
- [9] K. Symanzik, *Nucl. Phys.* B226, 187, 205 (1983); P. Hasenfratz, F. Niedermayer, *Nucl. Phys.* B414, 785 (1994).
- [10] B. Allés, A. Buonanno, G. Cella, *Nucl. Phys.* B500, 513 (1997).
- [11] A. A. Belavin, A. M. Polyakov, *JETP Letters* 22, 245 (1975).
- [12] A. Di Giacomo, F. Farchioni, A. Papa, E. Vicari, *Phys. Rev.* D46, 4630 (1992).
- [13] B. Berg, M. Lüscher, *Nucl. Phys.* B190, 412 (1981).
- [14] M. Campostrini, A. Di Giacomo, H. Panagopoulos, *Phys. Lett.* B212, 206 (1988).
- [15] A. Di Giacomo, E. Vicari, *Phys. Lett.* B275, 429 (1992); B. Allés, M. Campostrini, A. Di Giacomo, Y. Gündüç, E. Vicari, *Phys. Rev.* D48, 2284 (1993); F. Farchioni, A. Papa, *Nucl. Phys.* B431, 686 (1994).
- [16] M. Lüscher, *Commun. Math. Phys.* 85, 39 (1982).
- [17] U. Wolff, *Phys. Rev. Lett.* 62, 361 (1989).
- [18] R. Swendsen, J.–S. Wang, *Phys. Rev. Lett.* 58, 86 (1987).
- [19] P. G. Lauwers, V. Rittenberg, *Phys. Lett.* B233, 197 (1989).
- [20] J.–S. Wang, *Physica* A161, 249 (1989).

- [21] I. Dimitrovic, P. Hasenfratz, J. Nager, F. Niedermayer, Nucl. Phys. B350, 893 (1991).
- [22] C. M. Fortuin, P. W. Kasteleyn, Physica 57, 536 (1972).
- [23] J. Hoshen, R. Kopelman, Phys. Rev. B14, 3438 (1976).
- [24] D. Controzzi, G. Mussardo, Phys. Rev. Lett. 92, 021601 (2004); Phys. Lett. B617, 133 (2005); L. Campos Venuti et al., J. Stat. Mech. 0504, L02004 (2005).
- [25] A. S. Kronfeld, Nucl. Phys. (Proc. Suppl.) 17, 313 (1990); M. Lüscher, U. Wolff, Nucl. Phys. B339, 222 (1990).
- [26] G. Bhanot, F. David, Nucl. Phys. B251, 127 (1985).
- [27] M. P. Lombardo, Nucl. Phys. (Proc. Suppl.) 83, 375 (2000); A. Hart, M. Laine, O. Philipsen, Nucl. Phys. B586, 443 (2000); P. de Forcrand, O. Philipsen, Nucl. Phys. B642, 290 (2002); M. D'Elia, M. P. Lombardo, Phys. Rev. D67, 014505 (2003).